J Fluoresc (2011) 21:1439–1453
DOI 10.1007/s10895-010-0829-4

ORIGINAL PAPER

Binding Interactions of Toluidine Blue O with Escherichia Coli DNA: Formation of Bridged Structure

Malaichamy Ilanchelian · Ramasamy Ramaraj

Received: 7 July 2010 / Accepted: 29 December 2010 / Published online: 23 February 2011

Abstract The interaction(s) of Toluidine Blue O (TBO) with DNA was investigated using absorption and emission spectral methods. The binding of TBO with DNA was understood from the observed hypochromism in the absorption spectra and decrease in the emission intensity of TBO. From the absorption and emission spectral data, two binding constants were estimated for the binding of TBO with DNA. Based on the binding constant values both intercalative and electrostatic interactions of TBO with DNA were suggested. The TBO-DNA binding constant values reveal that the electrostatic interaction of TBO with DNA is weaker than the intercalative interaction. The emission quenching and salt effect studies showed that the TBO was partially intercalated with DNA. The two modes of binding between TBO and DNA may lead to the formation of bridging of a pair of DNA duplexes by TBO molecule. The electrostatic interaction is more important for the formation of the bridged structure of TBO with DNA. This was verified by studying the interaction of an anionic dye, Eosin Y (EY).

Keywords Bridged structure · Partial intercalation · Electrostatic binding · Toluidine blue O

Electronic supplementary material The online version of this article (doi:10.1007/s10895-010-0829-4) contains supplementary material, which is available to authorized users.

M. Ilanchelian
Department of Chemistry, Bharathiar University,
Coimbatore 641 046, India

R. Ramaraj (✉)
School of Chemistry, Madurai Kamaraj University,
Madurai 625 021, India
e-mail: ramarajr@yahoo.com

Introduction

Photoactive aromatic hydrocarbons, an important class of biologically active compounds, are mutagenic and carcinogenic and undergo physical and covalent interactions with deoxyribonucleic acid (DNA) [1–4]. The interactions of organic dyes with DNA have been widely studied in past three decades. The systematic investigation for the binding of metal complexes, porphyrins, natural antibiotics and other planar heterocyclic cations with DNA has revealed several structural and electronic factors that control the DNA binding affinity and sequence specificity of small molecules [5–8]. These studies were mainly carried out to understand the mechanism of anticancer drug action [5–9] to decipher the chemical basis for the carcinogenicity of environmental pollutants and toxic chemicals and to serve as analogues in the studies of protein-nucleic acid recognition [10]. This leads to the design of new and effective drugs against various deadly diseases [11]. Miniaturization of biosensors and biochips and fabrication of nanometric objects using a DNA template and DNA machines are some of the emerging fascinating applications in present day DNA research [12]. In general, drug molecules bind to DNA double helix by three binding modes: electrostatic, groove and intercalative [1–30]. Electrostatic interaction occurs between the negatively charged phosphate backbone of DNA double helix and the cationic or positive end of the polar drug. Groove binding involves hydrogen bonding or vander Waals interaction with the nucleic acid bases in the deep major groove or the shallow minor groove of the DNA double helix and finally, the intercalative binding intercalative binding, where the drug molecules intercalates itself into the base pairs of the DNA double helix. Among the three modes, intercalative binding is the most effective for drugs targeted to DNA. For investigating such binding

characteristics of the organic dyes to DNA, sensitive spectral techniques have been successfully exploited along with various other techniques. A non-negative charge on small drug molecules is considered as a necessary condition for the binding of drug molecules with DNA. Otherwise electrostatic repulsion between anionic DNA and the negatively charged drug molecules will affect interaction efficiency [21]. As a consequence of the biological significance, the spectroscopic properties of molecules containing amino and imino groups in the presence of DNA, in particular their absorption and emission behavior, have attracted much attention [5–7, 10–30].

The changing of spectroscopic and electrochemical properties of organic molecules, in particular, Toluidine Blue O (TBO), a phenothiazine dye by interacting with mediators and biological molecules is received arousing great interest in the fields of sensors and biosensors [31–35]. The redox and photochemical properties of TBO have also led to an increasing interest in photovoltaic devices because of their possible role as transducers of light to electric energy [36–38]. Several optical rotation and circular dichroism studies were made to obtain information on the phenomenon of helical aggregation of metachromatic dyes in the solution phase. These investigations have shown that TBO dye has a great ability to reveal the helical geometry of DNA-protein complexes as a consequence of molecular-ordered binding of TBO molecules on the DNA surface [39, 40].

DNA is an important target in the phenothiazinium dye-photosensitized biological damage, and guanine residues are particularly accessible [41–43]. Moreover, some phenothiazinium photosensitizers, such as TBO and methylene blue (MB), have found promising applications in photodynamic therapy of tumor [44–46]. These potential anti-tumor drugs can kill cancer cells through indirect or direct reactions with DNA [47].

To the best of our knowledge there are only limited investigations on the interaction of TBO with DNA have been reported. Resonance light scattering spectra of TBO in the presence of DNA indicated that TBO could aggregate along DNA surface [48]. Jiao et al., have studied the interaction of TBO with DNA by cyclic voltammetry and proposed the electrostatic binding of TBO with DNA [49]. Very recently, Yang et al., reported that the TBO interacts with DNA by both electrostatic and partial intercalation [50]. Although electrostatic, intercalative or both the interactions are proposed in the previous studies the interactions of the TBO with DNA was not completely understood. Thus in the present paper we have studied the interactions of TBO in the presence of DNA.

In this paper, we report the different binding modes of TBO with DNA including the electrostatic interaction in the absence of salts. The cationic TBO (Fig. 1) is expected to facilitate binding by electrostatic interaction with DNA double helix in addition to the partial intercalative interaction. The strong absorption and emission characteristics of TBO provide a sensitive spectroscopic handle to study its interaction with DNA. Further, the spectral data can be used to decipher the nature and strength of the stacking interaction between the chromophore and the DNA base pairs. A negatively charged dye, Eosin Y (EY) (Fig. 1), is also used to realize the importance of the electrostatic interaction of probes with DNA and the results are compared with TBO-DNA system.

Experimental Methods

Materials

TBO and EY (Aldrich) were purified by the reported procedures [51, 52]. Escherichia-coli (50% GC) DNA purified by phenol extraction [53] was used in this study.

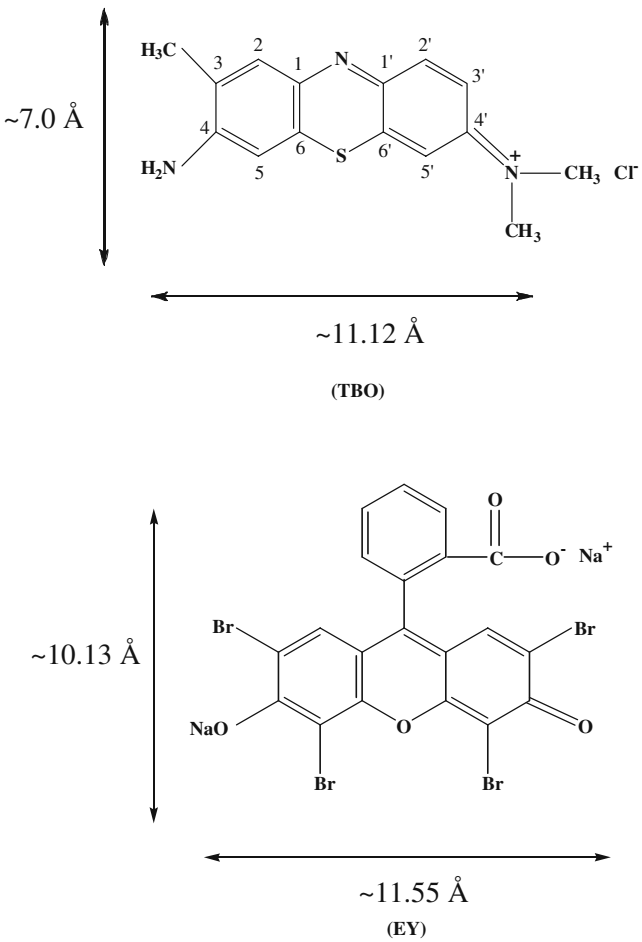

Fig. 1 Structure of Toluidine blue O (TBO) and Eosin Y (EY)

The purity of DNA was checked by monitoring the absorption and the ratio of absorbances at 260 and 280 nm was calculated as (≈1.9). The ratio indicated that the DNA was sufficiently free of protein [54]. The DNA, TBO and EY were dissolved in TE buffer pH 8 (10 mM Tris (Tris(hydroxymethyl) aminomethane-HCl) and 1 mM EDTA (Ethylene diamine tetra acetic acid) mixture). The DNA concentration per nucleotide (c(P)) was determined by absorption spectroscopy using the molar extinction coefficient value of 6600 $dm^3\ mol^{-1}\ cm^{-1}$ at 260 nm [55]. Other reagents were of analytical grade and used as received.

Spectral Measurements

Absorption spectral studies were carried out using a JASCO 7800 spectrophotometer. Emission studies were performed on a HITACHI F4500 fluorescence spectrophotometer. The TBO and EY were excited at 595 nm and 520 nm, respectively, and the emissions were monitored. The emission and excitation slit widths used throughout the experiment were 10 and 5 nm, respectively. The agarose gel electrophoresis scanning of TBO-DNA was run using a BIO-RAD wide mini-sub^{TM} cell. Electrophoresis was done at a constant voltage of 100 V for 1 h. Gel (1%) was stained in Ethidium bromide (EtBr) (0.5 μg/ml) solution for 30 min and visualized over a UV Trans-illuminator and photographed. The schematic model was created by Biosym-Insight II molecular modeling software on a silicon graphics computer system. All the measurements were carried out at room temperature (25°C). Water used in this investigation was doubly distilled over alkaline potassium permanganate using an all-glass apparatus. TBO and EY solutions (≈10^{-6} mol dm^{-3}) were always freshly prepared before use.

Results and Discussion

Absorption Spectral Studies of TBO with DNA

It has been well established that the binding of drug molecules with DNA helix has been characterized classically through absorption spectral titration by monitoring the changes in absorbance and shift in the wavelength [10, 21–29]. The absorption spectra of TBO (TE buffer pH 8) in the presence of different concentrations of DNA are shown in Fig. 2a. In the absence of DNA, TBO shows an absorption band at 624 nm (Fig. 2a(*a*)), which corresponds to the monomer TBO [38]. A decrease in the absorption intensity of TBO is observed (hypochromicity) upon increasing the concentration of DNA. For example, in the presence of 1.15 × 10^{-6} mol dm^{-3} of DNA, more than 50% decrease in absorption intensity of TBO was observed in addition to a small red shift from 624 to 629 nm. The observed hypochromism [56] indicates the presence of strong interactions between the DNA base pairs and TBO. A similar behavior has been reported for the metal complexes with salmon testes (ST) DNA [57] and RNA [58], phenazine dye with calf thymus DNA [27] and Thioflavin T with Escherichia coli DNA [59].

The binding constant of TBO with DNA is calculated by using Eq. 1 [60].

$$\frac{1}{\Delta A} = \frac{1}{(\varepsilon_1 - \varepsilon_0)[C_0]} + \frac{1}{(\varepsilon_1 - \varepsilon_0)[C_0]K_{bin}} \times \frac{1}{[DNA]} \qquad (1)$$

where ΔA is the difference in absorption intensities of TBO in the absence and presence of DNA (ΔA = (A_0 − A)), A_0

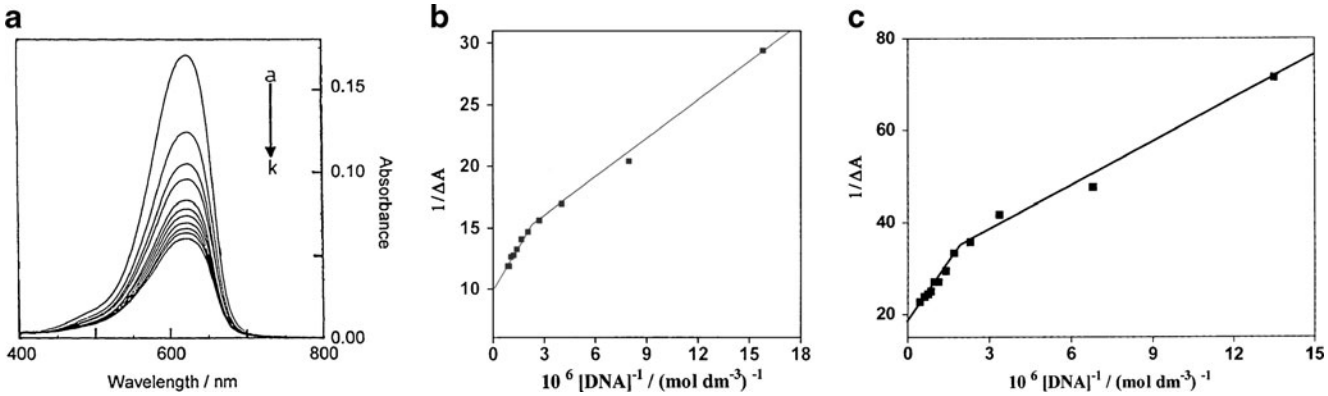

Fig. 2 **a** Absorption spectra of TBO (3.38×10^{-6} mol dm^{-3}) at various DNA concentrations. [DNA]: (*a*) 0, (*b*) 1.26×10^{-7}, (*c*) 2.49×10^{-7}, (*d*) 3.69×10^{-7}, (*e*) 4.88×10^{-7}, (*f*) 6.05×10^{-7}, (*g*) 7.19×10^{-7}, (*h*) 8.31×10^{-7}, (*i*) 9.41×10^{-7}, (*j*) 1.05×10^{-6} and (*k*) 1.15×10^{-6} mol dm^{-3}. **b** Double reciprocal plot obtained from the absorbance spectral data for the TBO-DNA system. **c** Double reciprocal plot obtained from the absorbance spectral data for the TBO-DNA system. [DNA] upto 5.18×10^{-6} mol dm^{-3}. [TBO]=1.38×10^{-6} mol dm^{-3}

is the absorption intensity of TBO in the absence of DNA, A is the absorption intensity of TBO at a given concentration of DNA, ε_1 and ε_0 are molar extinction coefficients of TBO and DNA, respectively. $[C_0]$ is initial concentration of TBO and K_{bin} is the binding constant. The double reciprocal plot of TBO-DNA system is shown in Fig. 2b. The plot is not linear as expected from Eq. 1. Most of the researchers have reported a linear plot for the binding of organic molecules with DNA [22, 27]. It has been suggested that the organic molecules intercalated into DNA giving a single binding constant value [22–29]. However, in the present study, Fig. 2b shows a non-linear plot consisting of two different regions, suggesting either the existence of two different species of TBO such as monomer and dimer or two different modes of binding interactions, there may be an intercalation or groove binding and electrostatic interactions for TBO with DNA.

In order to find out the non-linear plot is due to either the existence of two different species or two different binding modes. The absorption spectral observations of TBO in the presence of DNA are compared with our earlier work, the absorption spectral studies of γ-cyclodextrin (γ-CD) inclusion complexes of TBO [38]. When the concentration of γ-CD is increased the intensity of the absorption band due to monomer TBO at 624 nm is decreased with concomitant increase in the absorbance at 590 nm due to dimer TBO with an isosbestic point at 595 nm [38]. In contrast, when the concentration of DNA is increased only a decrease in the absorbance at 624 nm is observed and the band due to the dimer TBO at 590 nm is not observed. Further, we could not observe a dimer band for TBO at 590 nm even at high concentration of TBO (3.2×10^{-5} mol dm^{-3}) with DNA (Fig. not shown). The absence of TBO dimer band at 590 nm clearly rules out the possibility of existence of TBO dimer in the presence of DNA. Previously, we have reported a similar type of plot for the interaction of Thioflavin T (TFT) with Escherichia-coli DNA [59]. It leads to the existence of two different species for the interaction of TFT with DNA. In the present study, we could not observe such type of spectral changes for TBO with DNA. From the above results, we believe that the observed double reciprocal plot is due to the existence of two different modes of bindings between TBO and DNA.

The binding constant values are calculated from the intercept and slope of the non-linear plot and the values are given in Table 1 (Fig. 2b). The $K1_{bin}$ (at lower concentrations of DNA) values calculated for TBO-DNA are comparable to the binding constant values reported earlier for organic molecules with DNA, which is assigned to intercalative binding [21–29]. As a result, $K1_{bin}$ corresponds to the intercalative binding whereas $K2_{bin}$ (at higher concentrations of DNA) may correspond to another type of interaction, which is probably groove or electrostatic interaction of TBO with DNA.

Table 1 Binding constants of TBO with DNA using absorbance and emission spectral data

Spectral study	$K1_{bin}$[a]	$K2_{bin}$[a]
Absorption	11.45	3.08
Emission	10.65	2.63

[a] Binding constant $\times 10^6$ dm^3 mol^{-1}.

Average of three experimental values. pH=8 (TE buffer).

Binding constants can also be calculated from the Scatchard equation [61]. It is noted that the successful application of the Scatchard equation depends crucially an accurate determination of the amount of free dye ((i.e.,) not bound to DNA) in solution. This is difficult at lower DNA and higher dye concentrations and with strong binding constants ($\approx10^6$) and in these cases the use of the Scatchard equation is questionable [62]. In the present investigation we are unable to apply Scatchard equation to calculate the binding constant values using spectrophotometric data.

In the present investigation, the concentration of DNA was varied from 6.32×10^{-8} to 1.15×10^{-6} mol dm^{-3} (upto a [TBO]/[DNA] ratio≈3) (Fig. 2a & b) by keeping constant [TBO]=3.38×10^{-6} mol dm^{-3}. One would expect a maximal [TBO]/[DNA] ratio of 0.25 at saturation for intercalating dyes. We have also carried out absorption spectral measurements in the range of [DNA] (7.48×10^{-8} to 5.18×10^{-6} mol dm^{-3}) by keeping constant [TBO]=1.38×10^{-6} mol dm^{-3} ([TBO]/[DNA]≈0.27 (Fig. 2c)). In this case also we observed a non-linear double reciprocal plot (Fig. 2c). The observed double reciprocal plot (Fig. 2c) is very similar to one shown in Fig. 2b. Figure 2(b–c) also reveal that in addition to the intercalative interaction another type of interaction is also present between the TBO and DNA.

Very recently, Yang et al., reported that the TBO molecules can bind to DNA by both electrostatic and partial intercalation [50]. However, they could not observe non-linear plot for the interaction of TBO with DNA. The reason being, they have used high concentration range of DNA. In the present investigation, we have used the DNA concentration range from 6.32×10^{-8} to 1.15×10^{-6} mol dm^{-3}. However, when we used the DNA concentration range just above 4.88×10^{-7} mol dm^{-3} we could not observe the non-linear plot for the interactions of TBO with DNA. It indicates that the concentration range of DNA plays an important role for the interaction of TBO with DNA.

With the intention of identifying another type of interaction is whether groove binding or electrostatic interaction between TBO and DNA a strong electrolyte, sodium chloride (NaCl) was used. Earlier report clearly shows that higher concentrations of NaCl would hinder

small cationic molecules from binding with DNA [63]. The absorption spectra of TBO-DNA at different concentrations of NaCl are shown in Fig. 3. Figure 3 shows the absorption spectra of TBO-DNA solution at different concentrations of NaCl. As shown previously (Fig. 2a), a decrease in the absorption intensity was observed after the addition of DNA to TBO solution. However, the absorption intensity of TBO in the presence of DNA (Fig. 3*b*) was increased with increasing concentrations of NaCl (Fig. 3*c* and *d*) and attains a saturation after the addition of 0.3 mol dm^{-3} of NaCl (Fig. 3*e*). No further increase in the absorption intensity of TBO was observed if [NaCl] >0.25 mol dm^{-3}, which indicates that the NaCl could not completely release the binding of TBO from DNA (Fig. 3*e*). The increase in the absorption intensity of TBO is owing to the release of electrostatically bound TBO on the surface of the phosphate back bones of DNA by Na^+ ions (Fig. 3*c*–*d*). The attainment of saturation in the absorption intensity of TBO in the presence of DNA by the addition of NaCl is due to the inability to release the binding of the TBO molecules from DNA by NaCl (Fig. 3*e*). It is well known that when molecules intercalated into DNA base pairs, the double helix of DNA would protect them from external salts because of the presence of base pairs above and below the intercalator [27]. It is clearly indicate that in addition to the intercalation, electrostatic interaction also present in the TBO with DNA [64].

The absorption spectrum of Eosin Y (EY) in TE buffer (pH 8) solution shows an absorption band at 516 nm (see in the supportive information). The spectral changes observed for EY in the presence of different concentrations of DNA are shown in the supportive information. It can be shown that the absorption intensity of EY at 516 nm decreases (hypochromism) upon increasing the concentration of DNA. The observed decrease in the absorption intensity of the EY in the presence of DNA was much lower than that of TBO dye, for example only ~15% decrease in the absorption intensity was observed for EY in the presence of DNA. The binding constant value for the EY-DNA system is calculated from the absorption spectral data (see in the supportive information). In this case, the double reciprocal plot shows linear, it's indicating the existence of only one type of interaction between EY and DNA (see in the supportive information). This may be due to intercalative or groove or electrostatic interaction. The electrostatic interaction between the anionic EY and DNA is ruled out due to electrostatic repulsion between anionic EY and negatively charged phosphate back bone of DNA. The binding constant values clearly indicate that the interaction between EY and DNA is very weak (three orders of magnitude) compared to TBO-DNA system (Tables 1 and 2). The electrostatic repulsion between anionic EY and negatively charged phosphate back bone of DNA may be mainly responsible for the weak binding of the dye.

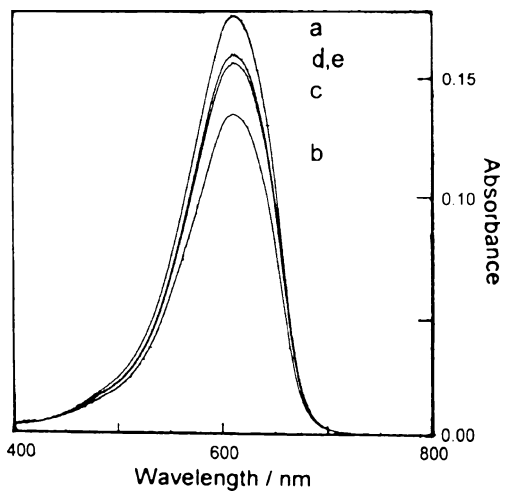

Fig. 3 Absorption spectra of TBO (3.4×10^{-6} mol dm^{-3}). (*a*): TBO alone and (*b*)–(*e*) : TBO in the presence of DNA (8.25×10^{-7} mol dm^{-3}). [NaCl]: (*b*) 0, (*c*) 0.125, (*d*) 0.25 and (*e*) 0.3 mol dm^{-3}

The absorption spectral changes of EY in the presence of DNA upon the addition of NaCl were also recorded and are shown in supportive information. It shows the absorption spectra of EY-DNA solution with increasing concentrations of NaCl. The absorption intensity of EY decreases with increasing concentrations of NaCl. As shown previously the addition of NaCl, resulted an increase in the absorption intensity for cationic TBO in the presence of DNA (Fig. 3). In the case of anionic EY, the absorption intensity of EY in the presence of DNA was decreased with increasing concentrations of NaCl (see in the supportive information). It is well known that when molecules intercalated into DNA base pairs, the double helix of DNA would protect them from external salts because of the presence of base pairs above and below the intercalator [27]. If EY molecules intercalate into DNA it should not be accessible to NaCl. However, the absorption spectral studies indicate that EY is accessible to NaCl because we observed a decrease in the absorption intensity with increase in the concentrations of

Table 2 Binding constants of EY with DNA (containing NaCl) using absorption spectral data

Spectral study	DNA containing NaCl[a]	$K1_{bin}$[b]
Absorption	0	9.37
	0.5	3.12
	3.0	2.27

[a] [NaCl]=mol dm^{-3}.

[b] Binding constant$\times10^3$ dm^3 mol^{-1}.

Average of three experimental values. pH=8 (TE buffer).

NaCl. Based on the above results we suggest that the intercalation of EY into DNA base pairs is not occurring. And also we could not observe the release of EY from the DNA binding upon the addition of NaCl due to the absence of electrostatic interaction between the anionic EY and the DNA phosphate backbone.

Previous study reported the copper complex of 2, 9-dimethyl-4,7-bis-(sulfonatophenyl)-1,10-phenanthroline with DNA [5]. They have found that the absorption intensity of the copper complex increases with increase in the concentrations of DNA [5]. It is due to the electrostatic interaction of negatively charged ligands on the phosphate back bone of the DNA with the help of Na^+ ions present in the buffer. However in our study we could not observe such type of spectral changes in the absorption spectral studies of EY with DNA. Hence, we concluded that the existing interaction between EY and DNA is groove binding [5].

Emission Spectral Studies of TBO with DNA

The interaction of TBO with DNA has also been studied by emission spectroscopy. The emission spectra recorded for TBO with different concentrations of DNA are shown in Fig. 4a. The emission spectrum of TBO in the absence of DNA shows an emission maximum at 630 nm, when TBO was excited at 595 nm [38]. The emission intensity of TBO at 630 nm was decreased upon increasing the concentrations of DNA show that TBO binds to DNA [21–29, 50]. The decrease in the emission intensity of TBO at 630 nm in the presence of DNA was analyzed using Stern-Volmer Eq. 2 [65].

$$\frac{I_f^0}{I_f} = 1 + K_{SV}[Q] \tag{2}$$

where I_f^0 and I_f are the emission intensities of TBO in the absence and presence of DNA. [Q] is the concentration of quencher and K_{SV} is the Stern-Volmer constant. The Stern-Volmer plot (Fig. 4a (Inset) shows deviation from linearity. The quenching curve tends towards the x-axis at higher concentrations of DNA. The changes in the emission spectra of TBO after adding DNA (Fig. 4a (Inset) indicates that there were strong interaction between TBO chromophore and the base pairs of DNA. Turro et al., have reported similar type of Stern-Volmer plot for the quenching of metal complexes with calf thymus DNA [66]. The extensive curvature observed in the Stern-Volmer plot has been attributed to the binding of metal complexes to DNA by both intercalative and electrostatic interactions. The quenching of thioflavin T with Escherichia Coli DNA system also we have reported similar type of Stern-Volmer plot [56]. It has been ascribed to the binding of thioflavin T to DNA by both groove and electrostatic interactions. Thus we presume that the curvature observed in the present study may also be due to the binding of cationic TBO molecule with DNA by both intercalative and electrostatic interactions. Data from emission titrations were also used to determine the binding constant of TBO with DNA by Eq. 3 [65].

$$\frac{I_f^0}{\Delta I_f} = \frac{1}{I_f^a K_{bin}[DNA]} + \frac{1}{I_f^a} \tag{3}$$

where ΔI_f is the difference in emission intensities of TBO in the absence and presence of DNA $\left(\Delta I_f = (I_f^0 - I_f)\right)$, I_f^0 is the emission intensity of TBO in the absence of DNA and I_f is the emission intensity of TBO at a given concentration of DNA), I_f^a is the fraction of the initial fluorescence which is accessible to quencher and K_{bin} is the binding constant. The double reciprocal plot (Fig. 4b) shows similar behavior as we have observed in the absorption spectral studies. The emission spectral studies also confirm the presence of two types of

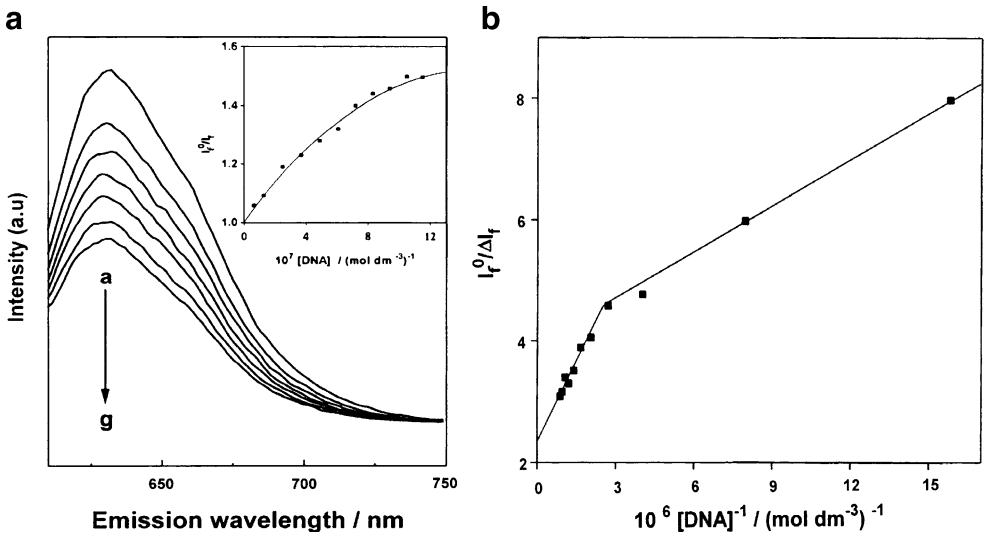

Fig. 4 **a** Emission spectra of TBO (3.4×10^{-6} mol dm^{-3}) at various DNA concentrations. [DNA]: (*a*) 0, (*b*) 6.32×10^{-8}, (*c*) 1.26×10^{-7}, (*d*) 2.49×10^{-7}, (*e*) 4.88×10^{-7}, (*f*) 7.19×10^{-7}, (*g*) 8.31×10^{-7} and (*h*) 1.15×10^{-6} mol dm^{-3}. (Inset) Plot of quenching of TBO (3.4×10^{-6} mol dm^{-3}) by DNA. **b** Double reciprocal plot obtained from the emission spectral data for the TBO-DNA system

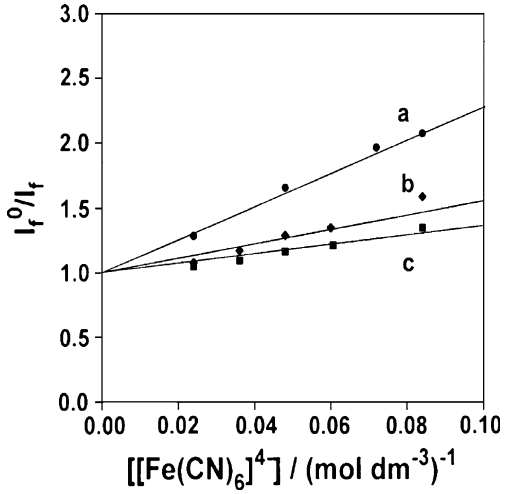

Fig. 5 Stern-Volmer plot for the quenching of TBO (3.4×10^{-6} mol dm^{-3}) by $[Fe(CN)_6]^{4-}$ in the absence (*a*) and presence of DNA. [DNA]=2.52×10^{-7} mol dm^{-3} (*b*) and 8.41×10^{-7} mol dm^{-3} (*c*) (λ_{ex}=590 nm and λ_{em}=630 nm)

binding between the TBO and DNA. The binding constant values are calculated from the intercept and slope of the plot and the values are given in Table 1.

The emission spectra of EY with increasing concentrations of DNA are also studied. The emission intensity of EY decreases with increasing concentrations of DNA (see in the supportive information). The observed decrease of emission intensity is due to the interaction of EY with DNA. In the emission spectral studies, we observed very similar behavior as observed in the absorption spectral studies.

Quenching Studies

In general, if small sensitizer molecules intercalate with DNA base pairs, the double helix of DNA would protect the sensitizer molecules from quenchers due to the presence of the base pairs above and below the intercalators [27]. In the present study the potassium ferrocyanide, an anionic quencher, is used to determine the relative accessibility of the TBO dye in the absence and presence of DNA [27]. The quenching studies were carried out for TBO in the absence and the presence of lower (2.52×10^{-7} mol dm^{-3}) and higher (8.41×10^{-7} mol dm^{-3}) concentrations of DNA with potassium ferrocyanide, respectively. The Stern-Volmer constant (K_{SV}) values of TBO are determined using Eq. 2 (Fig. 5). From the Stern-Volmer plot (Fig. 5), the K_{SV} values for the quenching of TBO-DNA by potassium ferrocyanide are calculated as 8.1 and 5.3 dm^3 mol^{-1} for the DNA concentrations of 2.52×10^{-7} and 8.41×10^{-7} mol dm^{-3}, respectively. In the absence of DNA, the K_{SV} value for TBO is calculated as 13.7 dm^3 mol^{-1} (Fig. 5). The K_{SV} values for TBO in the presence of DNA are lower than that of the K_{SV} value of TBO in the absence of DNA. As the DNA concentration increases from 2.52×10^{-7} to 8.41×10^{-7} mol dm^{-3}, the K_{SV} value decreases. This finding reveals that the available free dye in aqueous phase decreases with increasing the concentrations of DNA. Thus the K_{SV} value of TBO decreases at higher concentrations of DNA. When small molecules intercalate into DNA base pairs, the double helix DNA would protect them from quenchers, owing to the base pairs above and below the intercalator [27]. If that is the case, the fluorescence quenching of TBO might have completely suppressed after the addition of DNA. However, it can be seen from Fig. 5, quenching is not completely suppressed but only partially affected. These results support our postulation that TBO intercalates partially in to the DNA and the remaining part undergoes electrostatic interaction with the phosphate back bone of the DNA.

Absorption Spectral Studies of TBO with DNA Containing NaCl

To prove the partial intercalation of TBO with DNA by blocking the phosphate back bone of DNA using Na^+ ions as a result of adding NaCl. In this study we have used two types of DNA stock solutions containing 0.05 and 0.3 mol dm^{-3} of NaCl concentrations.

The absorption spectra of TBO in the presence of increasing concentrations of DNA containing 0.05 and 0.3 mol dm^{-3} concentrations of NaCl were studied. The absorption spectra of TBO in the presence of increasing concentrations of DNA containing 0.05 mol dm^{-3} of NaCl are shown in Fig. 6a. The absorption intensity of TBO decreases (Fig. 6a) (similar to TBO-DNA (Fig. 2a)) but attains a saturation at 1.15×10^{-6} mol dm^{-3} of DNA. The absorption spectra also recorded for TBO with increasing concentrations of DNA containing 0.3 mol dm^{-3} of NaCl are shown in Fig. 6b. The absorption intensity of TBO in the presence of DNA containing 0.3 mol dm^{-3} of NaCl (Fig. 6b) reaches the saturation even after the addition of 4.88×10^{-7} mol dm^{-3} of DNA.

The interaction of TBO with DNA containing NaCl is understood from the absorption spectral data using Eq. 1. Figure 6c shows the double reciprocal plots for TBO with DNA containing 0.05 and 0.3 mol dm^{-3} concentrations of NaCl. The double reciprocal plots of TBO with DNA showed a gradual change from non-linear to linear with increasing concentrations of NaCl in DNA (Fig. 6c). The binding constant values are calculated from the absorption spectral data of TBO at various concentrations of DNA containing 0.05 and 0.3 mol dm^{-3} of NaCl using Eq. 1 and the values are given in Table 3. In the absence of NaCl (Fig. 2b) and at lower concentrations of NaCl (0.05 mol dm^{-3}) in DNA (Fig. 6c), the double reciprocal plots are not linear whereas, at higher concentrations of NaCl (0.3 mol dm^{-3}) in DNA (Fig. 6c), the plot shows linear for TBO. This

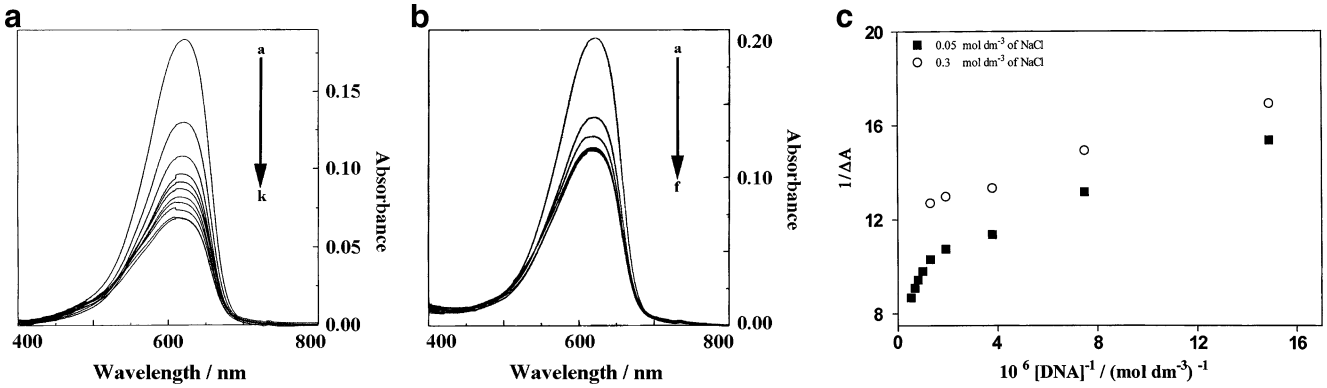

Fig. 6 **a** Absorption spectra of TBO (3.38×10^{-6} mol dm^{-3}) at various concentrations of DNA containing 0.05 mol dm^{-3} of NaCl. [DNA]: (*a*) 0, (*b*) 1.26×10^{-7}, (*c*) 2.49×10^{-7}, (*d*) 3.69×10^{-7}, (*e*) 4.88×10^{-7}, (*f*) 6.05×10^{-7}, (*g*) 7.19×10^{-7}, (*h*) 8.31×10^{-7}, (*i*) 9.41×10^{-7}, (*j*) 1.05×10^{-6} and (*k*) 1.15×10^{-6} mol dm^{-3}. **b** Absorption spectra of TBO (3.38×10^{-6} mol dm^{-3}) at various concentrations of DNA containing 0.3 mol dm^{-3} of NaCl. [DNA]: (*a*) 0, (*b*) 1.26×10^{-7}, (*c*) 2.49×10^{-7}, (*d*) 3.69×10^{-7}, (*e*) 4.88×10^{-7} and (*f*) 6.05×10^{-7}mol dm^{-3}. **c** Double reciprocal plot obtained from the absorption spectral data for TBO with DNA containing 0.05 and 0.3 mol dm^{-3} of NaCl

observation clearly indicates that the non-linear plots observed for cationic TBO in the absence and lower concentrations of NaCl in DNA show the existence of electrostatic interaction between TBO and DNA in addition to the partial intercalative interaction. On the other hand the linear plot obtained at higher concentrations of NaCl in DNA indicates the existence of partial intercalative interaction alone between the TBO and DNA. The absorption spectra recorded for the fixed concentration of 3.7×10^{-7} mol dm^{-3} of DNA containing 0.3 mol dm^{-3} of NaCl with increasing concentrations of NaCl are shown in Fig. 7. Figure 7(*a*) shows the absorption spectrum of TBO alone. The absorption intensity of TBO (Fig. 7(*a*)) decreases upon the addition of 3.7×10^{-7} mol dm^{-3} of DNA containing 0.3 mol dm^{-3} of NaCl (Fig. 7(*b*)) and the spectra shown in Fig. 7(*c*–*e*) are as a result of an increasing the concentration of NaCl. In these spectra we could not observe any change in the absorption spectra even after the addition of >0.25 mol dm^{-3} of NaCl (Fig. 7(*c*–*e*)). This indicates that the Na^+ ions block the electrostatic interaction between the TBO and DNA completely and the only interaction responsible for the decrease in the absorbance of TBO is the partial intercalative interaction. This clearly indicates that the TBO bound to DNA in the presence of 0.3 mol dm^{-3} of NaCl is partial intercalative in nature and it is inaccessible to the Na^+ ions even at higher concentrations of NaCl is added to the TBO-DNA solution.

The absorption spectra of EY in the presence of DNA containing 0.5 and 3.0 mol dm^{-3} of NaCl are shown in Fig. 8a and b. The absorption intensities of EY were decreased upon increasing the concentrations of DNA containing 0.5 and 3.0 mol dm^{-3} of NaCl (Fig. 8a and b). In contrast, we could not observe saturation effect for EY with DNA in the absorption spectra. The Na^+ ions facilitate the binding of EY with DNA in the presence of NaCl.

Table 3 Binding constants of TBO with DNA (containing NaCl) using absorption and emission spectral data

Spectral study	DNA containing NaCl[a]	$K1_{bin}$[b]	$K2_{bin}$[b]
Absorption	0	11.45	3.08
	0.3	10.89	–
Emission	0	10.65	2.63
	0.3	11.99	–

[a] [NaCl]=mol dm^{-3}.

[b] Binding constant$\times10^6$ dm^3 mol^{-1}.

Average of three experimental values. pH=8 (TE buffer).

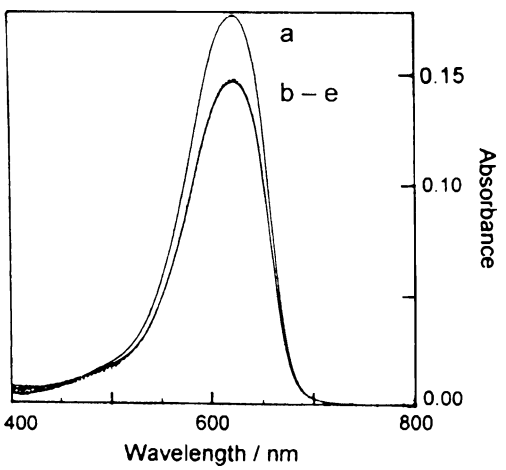

Fig. 7 Absorption spectra of TBO (3.4×10^{-6} mol dm^{-3}). (*a*): TBO alone and (*b*)–(*e*) : TBO containing DNA (3.7×10^{-7} mol dm^{-3}) containing 0.3 mol dm^{-3} NaCl. [NaCl]: (*b*) 0, (*c*) 0.125, (*d*) 0.25 and (*e*) 0.3 mol dm^{-3}

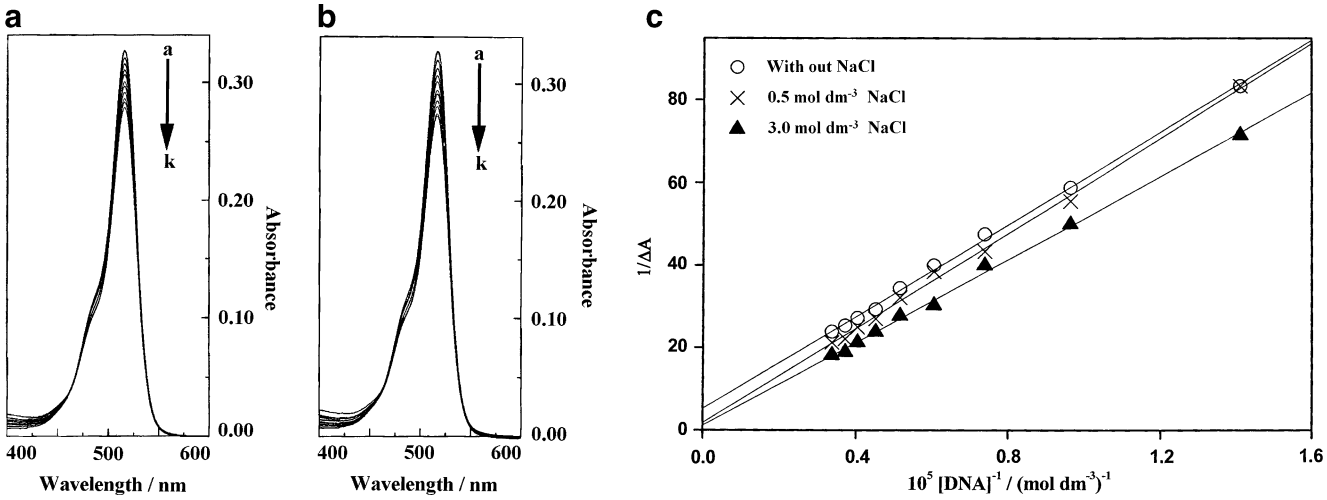

Fig. 8 **a** Absorption spectra of EY (3.36×10^{-6} mol dm^{-3}) at various concentrations of DNA containing 0.5 mol dm^{-3} of NaCl. [DNA]: (*a*) 0, (*b*) 3.63×10^{-6}, (*c*) 7.09×10^{-6}, (*d*) 1.04×10^{-5}, (*e*) 1.35×10^{-5}, (*f*) 1.65×10^{-5}, (*g*) 1.94×10^{-5}, (*h*) 2.22×10^{-5}, (*i*) 2.48×10^{-5}, (*j*) 2.74×10^{-5} and (*k*) 2.98×10^{-5} mol dm^{-3}. **b** Absorption spectra of EY (3.36×10^{-6} mol dm^{-3}) at various concentrations of DNA containing 3.0 mol dm^{-3} of NaCl. [DNA]: (*a*) 0, (*b*) 3.63×10^{-6}, (*c*) 7.09×10^{-6}, (*d*) 1.04×10^{-5}, (*e*) 1.35×10^{-5}, (*f*) 1.65×10^{-5}, (*g*) 1.94×10^{-5}, (*h*) 2.22×10^{-5}, (*i*) 2.48×10^{-5}, (*j*) 2.74×10^{-5} and (*k*) 2.98×10^{-5} mol dm^{-3}. **c** Double reciprocal plots obtained from the absorption spectral data of EY with DNA containing 0, 0.5 and 3.0 mol dm^{-3} of NaCl

The double reciprocal plots (Fig. 8c) which are derived from the absorption spectral studies of EY with DNA in the absence and presence of NaCl using Eq. 1 showed a single straight line for all the cases, when the concentration of NaCl was increased (Fig. 8c), there is no change in the linearity. From this study it is proposed that the binding of negatively charged EY with DNA is not electrostatic in nature.

Emission Spectral Studies of TBO with DNA Containing NaCl

The emission spectra of TBO in the presence of increasing concentrations of DNA containing 0.05 mol dm^{-3} of NaCl show a decrease in the emission intensity (Fig. 9a) similar to TBO with DNA in the absence of NaCl (Fig. 6a). However, the decrease in the emission intensity of TBO (Fig. 9b) reaches a saturation level upon increasing the concentrations of DNA containing 0.3 mol dm^{-3} of NaCl. The binding constant values are calculated from the emission spectral data of TBO at various concentrations of DNA containing 0.05 and 0.3 mol dm^{-3} of NaCl using Eq. 3 and the values are given in Table 3. Figure 9c shows the double reciprocal plots of TBO with increasing the concentration of DNA containing 0.05 and 0.3 mol dm^{-3} of NaCl. The double reciprocal plot (Fig. 9c) shows that the non-linear behavior changed to linear upon increasing the concentration of NaCl from 0.0 to 0.3 mol dm^{-3} in DNA.

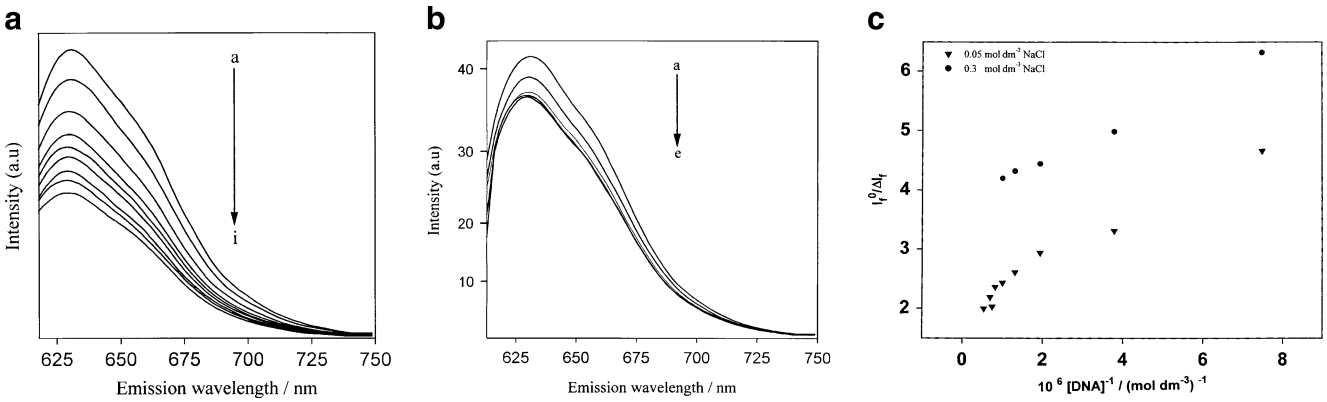

Fig. 9 **a** Emission spectra of TBO (3.4×10^{-6} mol dm^{-3}) at various concentrations of DNA containing 0.05 mol dm^{-3} NaCl. [DNA]: (*a*) 0, (*b*) 6.72×10^{-8}, (*c*) 1.34×10^{-7}, (*d*) 2.65×10^{-7}, (*e*) 5.19×10^{-7}, (*f*) 7.64×10^{-7}, (*g*) 1.22×10^{-6}, (*h*) 1.45×10^{-6} and (*i*) 1.86×10^{-6} mol dm^{-3}. λ_{ex}=595 nm. **b** Emission spectra of TBO (3.4×10^{-6} mol dm^{-3}) at various concentrations of DNA containing in 0.3 mol dm^{-3} NaCl. [DNA]: (*a*) 0, (*b*) 6.72×10^{-8}, (*c*) 1.34×10^{-7}, (*d*) 2.65×10^{-7} and (*e*) 1.01×10^{-6} mol dm^{-3}. λ_{ex}=595 nm. **c** Double reciprocal plot obtained from the emission spectral data for the TBO with DNA containing 0.05 and 0.3 mol dm^{-3} of NaCl

In the absence (Fig. 4b) and presence of 0.05 mol dm^{-3} of NaCl in DNA, the plots are not linear whereas, at 0.3 mol dm^{-3} of NaCl a linear plot is observed for the interaction of TBO with DNA(Fig. 9c). This result shows that one mode of binding disappears upon increasing the concentration of NaCl from 0.0 to 0.3 mol dm^{-3} in DNA. It indicates that the electrostatic interaction ($K2_{bin}$) between the TBO and DNA in the presence of NaCl is eliminated due to the repulsion between TBO and Na^+ ions present on the surface of phosphate back bones of DNA. Thus, intercalative ($K1_{bin}$) interaction alone exists between cationic TBO and DNA containing 0.3 mol dm^{-3} of NaCl [21–29]. From the above experiments, we suggest that both partial intercalation and electrostatic interactions are exist between the TBO and DNA in the absence and at lower concentrations of NaCl whereas purely partial intercalative interaction exists between TBO and DNA at higher concentrations of NaCl in DNA. Previously, it has been shown [5] that the presence of Na^+ ions on the surface of DNA favored the interaction of negatively charged ligands with DNA. In the present case, the presence of Na^+ ions on the surface of DNA repels the positively charged TBO ions from electrostatic binding to DNA. The interaction of salmon testes (ST) DNA and calf thymus DNA with metal complexes [5, 9] involve both partial intercalation and electrostatic interactions. These interactions lead to the formation of bridged structures in which one or more metal complexes link a pair of DNA duplexes together rather than engaging in classical intercalative binding [5, 9]. In the present investigation, we suggest that a similar type of interaction is present in the TBO-DNA binding. The schematic model of the partial intercalation and electrostatic interactions of TBO with DNA are shown in Fig. 10. The partial intercalation and electrostatic interactions may lead to form a bridged structure between TBO and DNA. The formation of bridged structure is possible because the TBO molecule is having a favorable length (11.12 Å) (Fig. 1). Part of the TBO molecules involves partial intercalation with DNA base pairs and the rest of the charge end is electrostatically interact with the phosphate back bone of DNA at higher concentrations of DNA will lead to the formation of bridged structure in which one or more TBO molecules link a pair of DNA duplexes together rather than engaging in classical intercalative binding.

Three Dimensional (3D) Emission Spectral Studies of TBO with DNA

The 3D emission spectra are recorded for TBO in the absence and presence of DNA. Figure 11a and b are showing the 3D emission spectra of TBO in the absence and presence of DNA. The contour intensity of TBO (Fig. 11a) decreases with increasing concentrations of DNA (Fig. 11b) due to the binding of TBO with DNA. This observation further confirms that the TBO molecules bind to DNA.

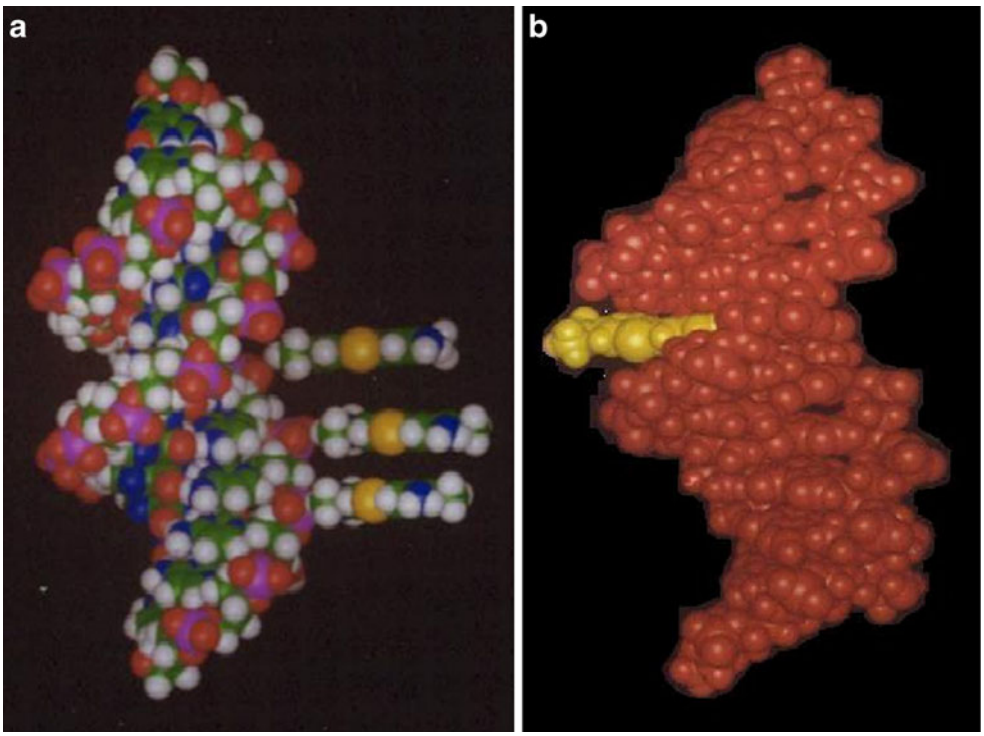

Fig. 10 **a** Schematic model of partial intercalative interaction between TBO and DNA. **b** Schematic model of electrostatic interaction between TBO and DNA

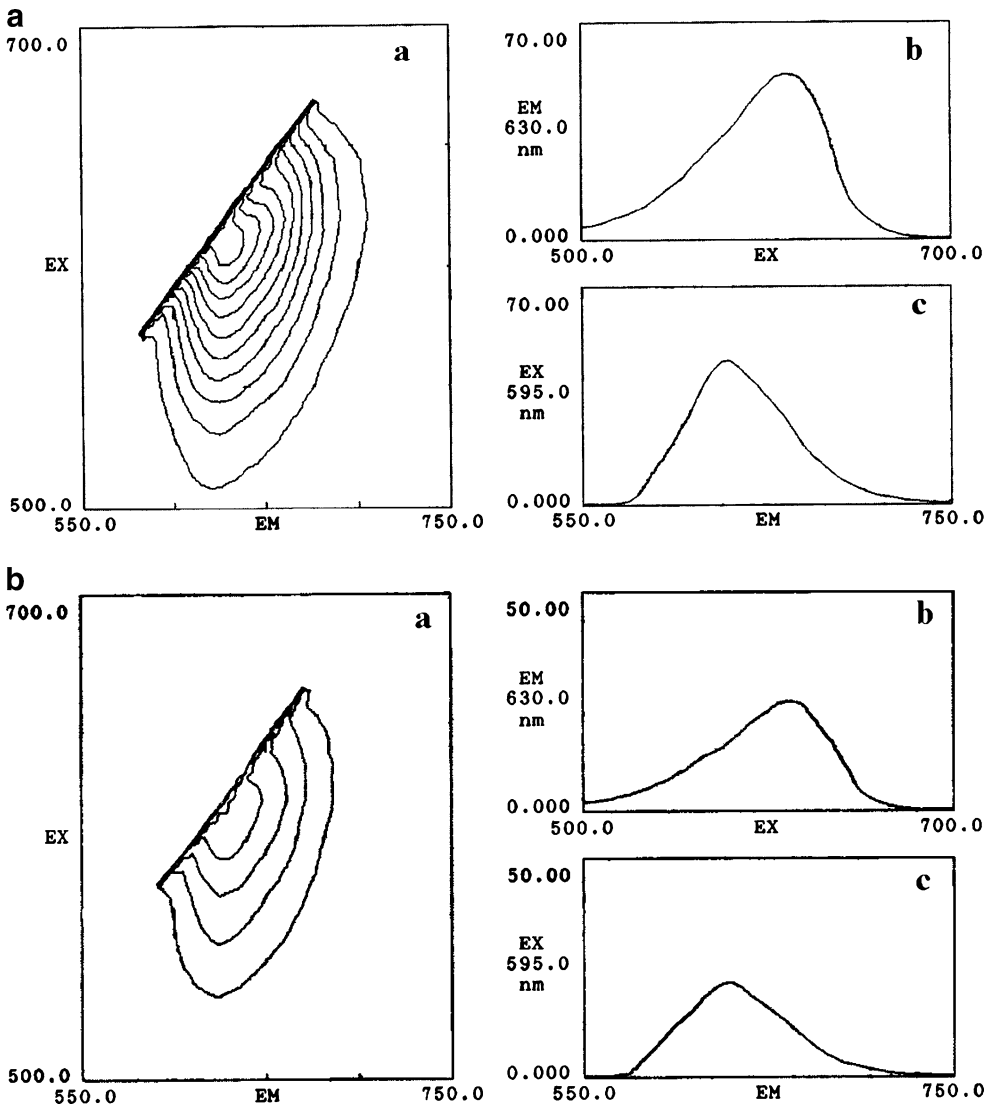

Fig. 11 **a** 3D emission spectra of TBO (3.4×10^{-6} mol dm^{-3}) in the absence of DNA. (*a*) Contour plot, (*b*) corresponding excitation spectrum and (*c*) emission spectrum. **b** 3D emission spectra of TBO (3.4×10^{-6} mol dm^{-3}) in the presence of 1.15×10^{-6} mol dm^{-3} of DNA. (*a*) Contour plot, (*b*) corresponding excitation spectrum and (*c*) emission spectrum

Gel Electrophoresis

Interaction of TBO with DNA was analyzed by agarose gel electrophoresis. Both supercoiled and linear forms of DNA were used for the gel electrophoresis. TBO, a positively charged molecule, migrates to the cathode when subjected to electrophoresis in buffer at pH 8, DNA being negatively charged moves in the opposite direction. If TBO binds strongly to DNA it is expected to co-electrophorese with the DNA and under the condition of low ionic strength it should reduce the electrophoretic mobility of the DNA. This effect was observed by increasing the concentration of TBO with linear DNA (Fig. 12, Lanes 5 to 2) and with supercoiled DNA (Fig. 12, Lanes 10 to 7). Lanes from right to left: 0.0001, 0.001, 0.01 and 0.1% of TBO solution containing 6.06×10^{-7} mol dm^{-3} of linear and supercoiled DNA, respectively (Fig. 12). The Lanes 1 and 6 are the references of linear and supercoiled DNA, respectively. The Lane 1 shows only one spot for the linear DNA whereas the Lane 6 shows three spots for supercoiled DNA due to the supercoiled, partially supercoiled or intermediate and relaxed forms (Fig. 12). Among the three forms, the supercoiled form is having a more comfortable structure and the mobility is higher as shown in the bottom spot of Lanes 6 and 10 (Fig. 12). When TBO alone migrate towards the cathode as a smear the path is observed easily from it's color. However, when DNA is mixed with lower concentrations of TBO, the path of TBO was not observed (Fig. 12, Lanes 4 & 5 and 9 & 10). At lower TBO concentrations almost all the TBO molecules are bound to DNA and the bound TBO molecules do not migrates towards the cathode. The streak (Lanes 3 & 2 and 8 & 7) in the gel represents the lower mobility of DNA due to TBO-DNA binding at higher concentrations of TBO (0.1 and 0.01% of TBO, respectively). Especially in the case of linear DNA, the spot in Lane 2 moves slower than the spot

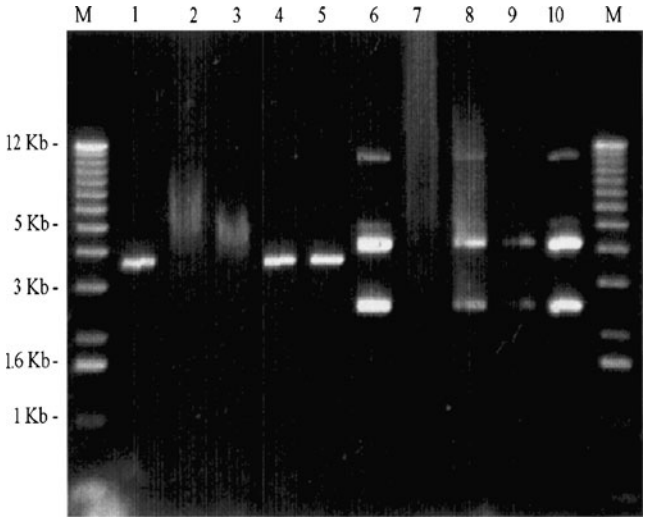

Fig. 12 Gel electrophoresis of TBO-DNA. Lane M: DNA Molecular weight marker. Lane 1: linear DNA alone (6.06×10^{-7} mol dm^{-3}). Lanes 2–5: 0.1, 0.01, 0.001 and 0.0001% of TBO with linear DNA (6.06×10^{-7} mol dm^{-3}), respectively. Lane 6: super coil DNA alone (6.06×10^{-7} mol dm^{-3}). Lanes 7–10: 0.1, 0.01, 0.001 and 0.0001% of TBO with super coil DNA (6.06×10^{-7} mol dm^{-3}), respectively

observed in Lane 3. This observation indicates that the TBO strongly binds to DNA. The gel electrophoresis study clearly shows that the cleavage of DNA duplexes was not occurred. The gel electrophoresis study also confirms the formation of bridged structure between TBO and DNA.

Model for TBO-DNA Interaction

To make up the model of molecules we should know the structure of the molecules. For solving the structure of TBO, we needed to combine information gathered from the previous structural studies of thiazine dyes. In particular, the previous reports on the structural studies of methylene blue (MB) and TBO molecules in the solid phase, showing similar chemical, structural, and photochemical properties [67–72].

The structural study on the MB dye was first performed by W.H. Taylor, who found a slight deformation of the molecule with the chloride ion close to the dimethylamino group [67]. The lack of planarity might probably be due to slight puckering of the molecule at the sulfur and nitrogen atoms bridging the two benzene rings.

The position of the chloride ion relative to the MB molecule has been the subject of discussion in the past. Zhdanov et al., concluded that the sulfur atom of the MB cation is close to the chloride ion (2.80 Å) because of the placement of the positive charge on the sulfur atom [68]. Marr et al. have shown that the chloride ion is close to the dimethylamino group at a distance of 4.12 Å by matching X-ray diffraction and Fourier electron density analyses [69, 70].

Bearing in mind these premises, Kahn-Harari et al., have reported the structural analysis of the toluidine blue sample was the crystal structural parameters of methylene blue [71]. A H atom replaced one methyl group at position 3, and methyl groups replaced two H atoms in position 2 for building up the model.

Recently, Caminiti et al., reported that the apparent structural differences between methylene blue and TBO geometry comparing the theoretical structural function with the experimental one in the range between 4.0 and 17.0 $Å^{-1}$ [72]. The calculation yielded a nonperfectly planar molecular configuration with the sulfur and nitrogen atoms of the heterocycle ring lying out of the molecular plane. The atomic Cartesian coordinates corresponding to that model has been reported [72]. The chloride ion interacts with the nitrogen atom of the dimethylamino group at a distance of 3.52±0.20 Å, showing a similar configuration to that reported by Marr et al. [69, 70]. The distance of the chloride ion with respect to the $N(CH_3)_2$ group is slightly different with respect to the MB. They have concluded that the structure of the single TBO molecule is slightly distorted and the chloride ion is closest to the dimethylamino group of the TBO cation.

Based on the recent report [72] we built the structures of TBO and the bridged structure formed between the TBO and DNA duplexes. Fig. 13 shows the formation of bridged

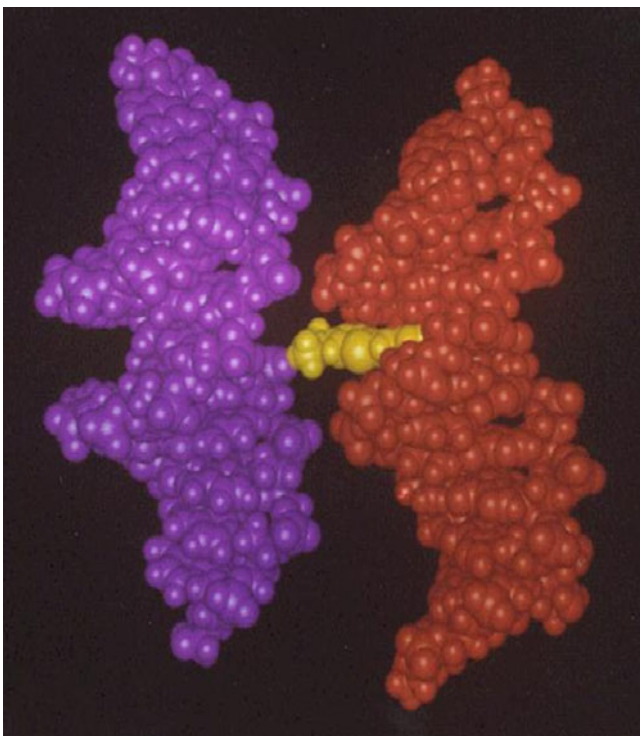

Fig. 13 Schematic model of the bridged structure formed between the TBO and DNA duplexes. One part of TBO bound to the DNA base pairs by intercalative interaction and another part of TBO (positively charged end) was bound on the surface of the DNA double helix by electrostatic interaction

structure between TBO and DNA. The model (Fig. 13) was built in such a way that it involves partial intercalation in to DNA base pairs (viz, the $-CH_3$ and $-NH_2$ groups) while the other left free end cationic = $N^+(CH_3)_2$ group of the TBO is involved the electrostatic interaction with the phosphate back bones of DNA.

The structure of TBO suggested in the present work are quite different from those of Wang and Yang's multiplex binding modes of toluidine blue with Calf thymus DNA study [50]. These authors suggested that the TBO partially intercalated into calf thymus DNA with the molecular plane preferably inserting into DNA base from the ring $C_1'NC_1$ side. The discrepancy between their suggestion and ours can be attributed to the difference in the partial intercalation and electrostatic interaction scheme.

Conclusion

The present study supported the possibility of both partial intercalation and electrostatic interactions are present for the interaction of TBO with DNA. To the best of our knowledge, for the first time we clearly demonstrated the formation of bridged structure formed between an organic dye (TBO) with DNA with the help of both partial intercalation and electrostatic interactions. The electrostatic interaction of TBO with DNA is quite important for the formation of TBO-DNA bridged structure. In the absence of such additional interaction involving the TBO domain, only partial intercalative interaction is possible. The quenching studies clearly indicated that the TBO molecule is deeply buried in the DNA by partial intercalation. The addition of NaCl to TBO-DNA solution clearly showed the presence of partial intercalative binding as well as electrostatic interaction between TBO and DNA. The anionic EY-DNA system showed that the electrostatic interaction is absent and the binding between the EY and DNA is weaker than the cationic TBO with DNA. The present study showed that a molecular system based on the phenothiazine chromophore can be designed to study the bridged structure formed between the DNA and small cationic organic molecule.

Acknowledgements Financial support from the Department of Science and Technology (DST) is gratefully acknowledged. We thank Dr. R. Usha, School of Biotechnology for providing DNA samples and Dr. Z.A. Rafi and The National Center for High-Resolution Graphics, Bioinformatics, Madurai Kamaraj University for the help to create the schematic Model TBO-DNA.

References

1. Heidelberger C (1975) Chemical carcinogenesis. Annu Rev Biochem 44:79–121
2. Wolfe A, Shimer GH Jr, Meehan T (1987) Polycyclic aromatic hydrocarbons physically intercalate into duplex regions of denatured DNA. Biochemistry 26(20):6392–6396
3. VYa S, Dourandin A, Luneva NP, Geacintov NE (1997) Migration and trapping of photoinjected excess electrons in double-stranded B-form DNA but not in single-stranded DNA. J Phys Chem B 101 (30):5863–5868
4. Wirth M, Buchardt O, Koch T, Nielsen PE, Norden B (1988) Interactions between DNA and mono-, bis-, tris-, tetrakis-, and hexakis(aminoacridines). A linear and circular dichroism, electric orientation relaxation, viscometry, and equilibrium study. J Am Chem Soc 110(3):932–939
5. Mahadevan S, Palaniandavar M (1998) Spectroscopic and voltammetric studies on copper complexes of 2, 9-dimethyl-1, 10-phenanthrolines bound to calf thymus DNA. Inorg Chem 37 (4):693–700
6. Waring MJ (1977) In: Roberts GCK (ed) Drug action at the molecular level. Macmillan, London, pp 167–189
7. Porschke D (1986) In: Gushlballer W, Saenger W (eds.) DNA-ligand, interactions specificity, dynamics of protein-nucleic acid interactions, p. 85
8. Barton JK (1983) Tris(phenanthroline) metal complexes: probes for DNA helicity. J Biomol Struct Dyn 1(3):621–632
9. Liu F, Meadows KA, McMillin DR (1993) DNA-binding studies of $Cu(bcp)_2^+$ and $Cu(dmp)_2^+$: DNA elongation without intercalation of $Cu(bcp)_2^+$. J Am Chem Soc 115(15):6699–6704
10. Kelly JM, Murphy MJ, McConnell DJ, OhUigin C (1985) A comparative study of the interaction of 5, 10, 15, 20-tetrakis (N-methylpyridinium-4-yl)porphyrin and its zinc complex with DNA using fluorescence spectroscopy and topoisomerisation. Nucleic Acid Res 13(1):167–184
11. Dervan PB (2001) Molecular recognition of DNA by small molecules. Bioorg MedChem 9:2215–2235
12. Ganguli M, Jayachandran KN, Maiti S (2004) Nanoparticles from cationic copolymer and DNA that are soluble and stable in common organic solvents. J Am Chem Soc 126(1):26–27
13. Will G, Kudryashov E, Duggan E, Fitzmaurice D, Buckin V, Waghorne E, Mukherjee S (1999) Excited state complex formation between 3-aminophthalhydrazide and DNA: a fluorescence quenching reaction. Spectrochim Acta A 55(13):2711–2717
14. Sigman DS, Graham DR, Aurora VD, Stern AM (1979) Oxygen-dependent cleavage of DNA by the 1, 10-phenanthroline cuprous complex. Inhibition of Escherichia coli DNA polymerase I. J Biol Chem 55(24):12269–12272
15. Spassky A, Sigman DS (1985) Nuclease activity of 1, 10-phenanthroline-copper ion. Conformational analysis and foot-printing of the lac operon. Biochemistry 24(27):8050–8056
16. Sigman DS (1986) Nuclease activity of 1, 10-phenanthroline-copper ion. Acc Chem Res 19(6):180–186
17. Hirao T, Nomoto A, Yamazaki S, Ogawa A, Moriuchi T (1998) Aggregation of ferrocene pendant groups along the backbone of DNA for a supramolecular redox system. Tetrahedron Lett 39 (24):4295–4298
18. Takenaka S, Uto Y, Saita H, Yokoyama M, Honda H, Wilson WD (1998) Electrochemically active threading intercalator with high double stranded DNA selectivity. J Chem Soc Chem Commun 1111–1112.
19. Neelakandan PP, Hariharan M, Ramaiah D (2006) A Supramolecular ON−OFF−ON fluorescence assay for selective recognition of GTP. J Am Chem Soc 128(35):11334–11335
20. Sugiyama H, Lian C, Isomura M, Saito I, Wang AHJ (1996) Distamycin A modulates the sequence specificity of DNA alkylation by duocarmycin A. Proc Natl Acad Sci USA 93 (25):14405–14410
21. Friedmann T, Brown DM (1978) Base-specific reactions useful for DNA sequencing: methylene blue—sensitized photooxidation of

guanine and osmium tetraoxide modification of thymine. Nucleic Acid Res 5(2):615–622
22. Brun AM, Harriman A (1992) Dynamics of electron transfer between intercalated polycyclic molecules: effect of interspersed bases. J Am Chem Soc 114(10):3656–3660
23. Shaw AK, Pal SK (2007) Fluorescence relaxation dynamics of acridine orange in nanosized micellar systems and DNA. J Phys Chem B 111(16):4189–4199
24. Ito F, Kakiuchi T, Nagamura T (2007) Excitation energy migration of acridine orange intercalated into Deoxyribonucleic Acid thin films. J Phys Chem C 111(19):6983–6988
25. Waring MJ (1965) Complex formation between ethidium bromide and nucleic acids. J Mol Biol 13(1):269–282
26. Banerjee D, Pal SK (2007) Simultaneous binding of minor groove binder and intercalator to dodecamer DNA: Importance of relative orientation of donor and acceptor in FRET. J Phys Chem B 111 (19):5047–5052
27. Cao Y, He Xi-Wen (1998) Studies of interaction between safranine T and double helix DNA by spectral methods. Spectrochim Acta A 54(6):883–892
28. Sarkar DP, Basak S, Chattopadhyay N (2008) Binding interaction of cationic phenazinium dyes with Calf Thymus DNA: a comparative study. J Phys Chem B 112(30):9243–9249
29. Tuite E, Norden B (1994) Sequence-specific interactions of methylene blue with polynucleotides and DNA: a spectroscopic study. J Am Chem Soc 116(17):7548–7556
30. Rohs R, Sklenar H, Lavery R, Röder B (2000) Methylene blue binding to DNA with alternating GC base sequence: a modeling study. J Am Chem Soc 122(12):2860–2866
31. Chen S, Yuan R, Chai Y, Xu L, Wang N, Li X, Zhang L (2006) Amperometric hydrogen peroxide biosensor based on the immobilization of horseradish peroxidase (HRP) on the layer-by-layer assembly films of gold colloidal nanoparticles and toluidine blue. Electroanalysis 18(5):471–477
32. Jiao K, Li QJ, Sun W, Wang Z (2005) Voltammetric detection of the DNA interaction with toluidine blue. Electroanalysis 17 (11):997–1002
33. Tian F, Zhu G (2004) Toluidine blue modified self-assembled silica gel coated gold electrode as biosensor for NADH. Sens Actuators B 97(1):103–108
34. Ribeiro ES, Dias SLP, Fujiwara ST, Gushichem Y, Bruns RE (2003) Electrochemical study and complete factorial design of toluidine blue immobilized on SiO_2/Sb_2O_3 binary oxide. J Appl Electrochem 33(11):1069–1075
35. Ju H, Xiao Y, Lu X, Chen H (2002) Electrooxidative coupling of a toluidine blue O terminated self-assembled monolayer studied by electrochemistry and surface enhanced Raman spectroscopy. J Electroanal Chem 518(2):123–130
36. Jana AK (2000) Solar cells based on dyes. J Photochem Photobiol A 132(1):1–17
37. Gangotri KM, Meena RC, Meena R (1999) Use of micelles in photogalvanic cells for solar energy conversion and storage: cetyl trimethyl ammonium bromide-glucose-toluidine blue system. J Photochem Photobiol A 123(1–3):93–97
38. Ilanchelian M, Retna Raj C, Ramaraj R (2000) Spectral studies on the cyclodextrin inclusion complexes of toluidine blue o and meldola's blue in aqueous solution. J Incl Phenom Macro Chem 36(1):9–20
39. Prento P (2001) A contribution to the theory of biological staining based on the principles for structural organization of biological macromolecules. Biotech Histochem 76(3):137–161
40. De Campos VB (2000) Extended chromatin fibres: crystallinity, molecular order and reactivity to concanavalin-a. Cell Biol Int 24 (10):723–728
41. Dohno C, Stemp EDA, Barton JK (2003) Fast back electron transfer prevents guanine damage by photoexcited thionine bound to DNA. J Am Chem Soc 125(32):9586–9587
42. Reid GD, Whittaker DJ, Day MA, Turton DA, Kayser V, Kelly JM, Beddard GS (2002) Femtosecond electron-transfer reactions in mono- and polynucleotides and in DNA. J Am Chem Soc 124 (19):5518–5527
43. Kelly JM, van der Putten WJ, McConnell DJ (1987) Laser flash spectroscopy of methylene blue with nucleic acids. Photochem Photobiol 45(2):167–175
44. Rohs R, Sklenar H, Lavery R, Roder B (2000) Methylene blue binding to DNA with alternating GC base sequence: a modeling study. J Am Chem Soc 122(12):2860–2866
45. Harris F, Chatfield LK, Phoenix DA (2005) Phenothiazinium based photosensitisers—photodynamic agents with a multiplicity of cellular targets and clinical applications. Curr Drug Target 6 (5):615–627
46. Tremblay JF, Dussault S, Viau G, Gad F, Boushira M, Bissonnette R (2002) Photodynamic therapy with toluidine blue in Jurkat cells: cytotoxicity, subcellular localization and apoptosis induction. Photochem Photobio Sci 1(11):852–856
47. Tuite EM, Kelly JM (1993) New trends in photobiology: photochemical interactions of methylene blue and analogues with DNA and other biological substrates. J Photoch Photobio B 21(2–3):103–124
48. Chen LH, Nie YT, Liu LZ, Shen HX (2003) Determination of nucleic acids on the basis of enhancement effect of resonance light scattering of toluidine blue. Anal Lett 36(1):107–122
49. Jiao K, Li QJ, Sun W, Wang ZJ (2005) Voltammetric detection of the DNA interaction with toluidine blue. Electroanal 17(11):997–1002
50. Wang J, Yang X (2009) Multiplex binding modes of toluidine blue with calf thymus DNA and conformational transition of DNA revealed by spectroscopic studies. Spectrochim Acta A 74 (2):421–426
51. Gopidas KR, Kamat PV (1990) Photochemistry in polymers: photoinduced electron transfer between phenosafranine and triethylamine in perfluorosulfonate membrane. J Phys Chem 94 (11):4723–4727
52. Jines J II, Chatterjee S (1988) Steric control of distance parameters and the yield of charge carriers in photochemical electron transfer. The quenching of eosin Y by hindered phenols. J Phys Chem 92(24):6862–6864
53. Maniatis T, Fritsch EF, Sambrook J (1982) Molecular cloning: A laboratory manual. Cold Spring Harbor, New York, pp 458–460
54. Marmur J (1961) A procedure for the isolation of deoxyribonucleic acid from micro-organisms. J Mol Biol 3(2):208–218
55. Reichmann ME, Rice SA, Thomas CA, Doty P (1954) **A** further examination of the molecular weight and size of desoxypentose Nucleic Acid. J Am Chem Soc 76(11):3047–3053
56. Long EC, Barton JK (1990) On demonstrating DNA intercalation. Acc Chem Res 23(9):271–273
57. Tamilarasan R, Mc Millin DR (1990) Photophysical studies of copper phenanthrolines bound to DNA. Inorg Chem 29(15):2798–2802
58. Waring MJ (1981) DNA modification and cancer. Ann Rev Biochem 50:159–192
59. Ilanchelian M, Ramaraj R (2004) Emission of thioflavin T and its control in the presence of DNA. J Photochem Photobiol A Chem 162(1):129–137
60. Hamai S (1982) Association of inclusion compounds of β-cyclodextrin in aqueous solution. Bull Chem Soc Jpn 55 (9):2721–2729
61. Van Holde KE (1985) In: Physical biochemistry. Prentice-Hall, Englewood Cliffs NJ, pp. 197–199
62. Kelly JM, Lyons MEG, Van der putten WJM (1986) In: Smyth MR, Vos JG (eds), Electrochemistry, sensors and analysis. Elsevier Science Publishers, BV Amsterdam, Netherlands. 25:205–213

63. Prativel G, Bermadou J, Meunier B (1995) Carbon–hydrogen bonds of DNA sugar units as targets for chemical nucleases and drugs. Angew Chem Int Ed Engl 34:746–769
64. Pyle AM, Rehmann JP, Meshoyrer R, Kumar CV, Turro NJ, Barton JK (1989) Mixed-ligand complexes of ruthenium(II): factors governing binding to DNA. J Am Chem Soc 111 (8):3051–3058
65. Lakowicz JR (2006) Principles of fluorescence spectroscopy, 3rd edn. Springer, New York, pp 280–289
66. Kumar CV, Barton JK, Turro NJ (1985) Photophysics of ruthenium complexes bound to double helical DNA. J Am Chem Soc 107(19):5518–5523
67. Taylor WHZ (1935) An X-ray examination of methylene blue. Krystallogr 91:450–460
68. Zhdanov GS, Zvonkova ZV, Vorontsova LG (1956) X-ray structural study of a methylene blue dye. Sov Phys Crystallogr 1:44–48
69. Marr III HE, Stewart JM (1971) The crystal structure of methylene blue. Chem Commun 131
70. MarrIII HE, Stewart JM, Chiu MF (1973) The crystal structure of methylene blue pentahydrate. Acta Crystallogr B 29:847–853
71. Kahn-Harari A, Ballare RE, Norris EK (1973) The crystal structure of methylene blue thiocyanate. Acta Crystallogr B 29 (4):1124–1126
72. Matassa R, Sadun C, D'Ilario L, Martinelli A, Caminiti R (2007) Supramolecular organization of toluidine blue dye in solid amorphous phases. J Phys Chem B 111(8):1994–1999